

Digital circuits using self-shunted Nb/Nb_xSi_{1-x}/Nb Josephson junctions

David Olaya,^{1,a)} Paul D. Dresselhaus,¹ Samuel P. Benz,¹ Anna Herr,² Quentin P. Herr,² Alexander G. Ioannidis,² Donald L. Miller,² and A. W. Kleinsasser³

¹National Institute of Standards and Technology, Boulder, Colorado 80305, USA

²Northrop Grumman Corporation, Linthicum, Maryland 21203, USA

³Jet Propulsion Laboratory, Pasadena, California 91109, USA

(Received 5 February 2010; accepted 29 April 2010; published online 27 May 2010)

Superconducting digital circuits based on Josephson junctions with amorphous niobium-silicon (a-NbSi) barriers have been designed, fabricated, and tested. Single-flux-quantum (SFQ) shift registers operated with $\pm 30\%$ bias margins, confirming junction reproducibility and uniformity. Static digital dividers operated up to 165 GHz for a single value of bias current, which was only marginally slower than circuits fabricated with externally shunted AlO_x-barrier junctions having a comparable critical current density of 4.5 kA/cm². In comparison, self-shunted a-NbSi junctions enabled a doubling in circuit density. This and their relatively thick 10 nm barriers could increase the yield of complex SFQ circuits. © 2010 American Institute of Physics. [doi:10.1063/1.3432065]

Josephson junctions are the basis for superconducting electronics. Their exceptional properties, including terahertz cut-off frequency, low power dissipation, and low noise, have found many applications in metrology, mixed-signal circuits, radiation detectors, and magnetic sensors. Superconducting single-flux-quantum (SFQ) technology realizes unprecedented high-speed and low-power operation.¹

Currently, most superconducting digital circuits are based on Nb/AlO_x/Nb Josephson junctions.² They have demonstrated good uniformity and reproducibility on a scale of 10 000 or more junctions per chip.^{3,4} However, the maximum operating frequency of such circuits is an order of magnitude lower than circuits with a small number of similar junctions.⁵ One limitation of this type of junction may be imposed by the thin (~ 1 nm) tunnel barrier. A typical Nb/Al–AlO_x/Nb device has a critical current density (J_c) of 4.5 kA/cm². Devices with $J_c=20$ kA/cm² approach a potential practical limit for AlO_x,⁶ as transport becomes increasingly dominated by barrier defects as it is thinned to increase J_c . Tunnel junctions have a high intrinsic capacitance and require external shunting in order to reduce the RC time constant. This increases the complexity of the fabrication process and circuit layout, and reduces circuit density. These limitations are avoided in self-shunted junctions, hence the diverse efforts to make them include SNS (N = normal metal) junctions with high-resistivity barrier materials such as TiN_x, NbN_x and TaN_x, and SNIS and SINIS junctions, with Al and AlO_x as normal metals and insulators, respectively. For the latter, simple SFQ circuits have been demonstrated.⁷

For similar J_c , a NbSi barrier is nearly ten times thicker than an AlO_x tunnel barrier in SIS and SINIS junctions. If effects such as surface roughness or pinholes are limiting junction uniformity, junctions with thicker barriers should have better uniformity, leading to better circuit yield. Indeed, NbSi junctions have been demonstrated in voltage standard devices with 70 000 junctions with much better yield than similar circuits using SINIS junctions.⁸

The electrical characteristics of NbSi-barrier junctions are tunable due to the fact that the barrier is formed by co-sputtering Si and Nb. By independently controlling the composition (through the relative sputtering rates) and the thickness, a large range of values for the junction properties may be obtained, enabling these junctions to be used in a wide range of circuits and applications.⁹

The NbSi films of interest for SFQ circuits are on the insulating side of the metal-insulator transition. In this regime, flexible control of the barrier dissipation and capacitance is possible by changing its composition and thickness. For instance, it is possible to have junctions with the same J_c but different I_cR values (I_c is the critical current and R is the effective resistance of the junction). Likewise, it is possible to have junctions with different J_c s while having the same I_cR product.¹⁰ These junctions can be made to be intrinsically critically damped over a wide range of J_c s. The co-sputtered deposition process is simple and requires no intermediate oxidation steps. The barrier materials can also be dry-etched with the same process as that for the Nb electrodes. These features were exploited to produce uniform arrays of double- and triple-stacked junctions for voltage standard circuits.¹¹ Higher-density SFQ circuits may also be possible by use of this simple fabrication process.

The two SFQ circuits we measured were a static digital divider and a 16-bit shift register. The divider circuit is the industry standard for determining the speed of a digital technology.^{5,12} The shift register is a standard circuit for verifying junction reproducibility and yield. Both circuits were designed using conservative 2 μm design rules for the interconnects and 1.5 μm smallest junction diameter, similar to the typical design rules used for 4.5 kA/cm² Nb/AlO_x/Nb processes.¹³

The two wafers presented here were intentionally fabricated to have nearly the same J_c of 5.5 kA/cm², but different junction resistances in order to study the effective damping of NbSi junctions in digital circuits. Junctions in wafer I had 10.8 nm thick barriers deposited with 16/200 W of Nb/Si sputter powers, while wafer II had 9.6 nm barriers with 15/200 W of Nb/Si sputter powers.

Figure 1 shows the dc I - V curves of a $2.5 \times 2.5 \mu\text{m}^2$ square junction from wafer I at 4.2 K, without and with

^{a)}Electronic mail: david.olaya@nist.gov.

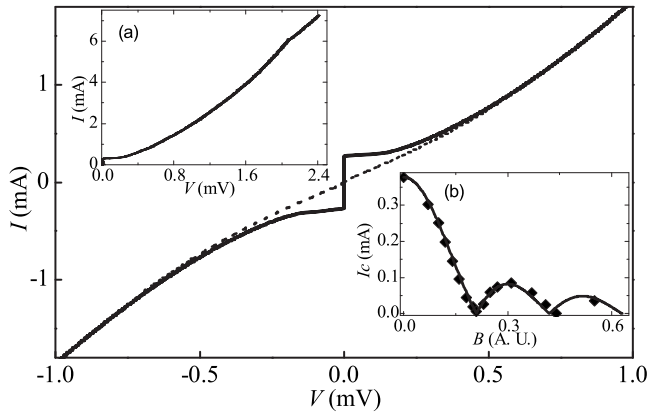


FIG. 1. I - V characteristic of a junction from wafer I at 4.2 K. The dashed curve corresponds to the first I_c minimum in applied magnetic field. Inset (a) is the zero-field curve up to higher currents. Inset (b) shows the Fraunhofer pattern of a similar junction with a 10.4 nm thick, 16/200 W NbSi-barrier.

suppression of the Josephson I_c by a magnetic field parallel to the film plane. No hysteresis is observed. An indication of the uniformity of the NbSi barriers in this work is the nearly ideal Fraunhofer patterns (I_c variation with applied field) observed, with I_c nearly completely suppressed. The I_c -suppressed I - V curves are nonlinear.

The nonlinearity below ~ 1 mV in Fig. 1 is of interest for digital circuits and needs to be further investigated. It is likely that the conduction through the barrier, which is near a metal-insulator transition, is intrinsically nonlinear. The dynamic resistance of the I - V curve below the gap voltage is generally higher than the linear resistance (R_n) that is measured above the gap. This means that the effective characteristic voltage, $V_c = I_c R$, for digital circuit applications is higher than estimates based on R_n .

The quality factors of both junctions were estimated from the amount of hysteresis in the curves.¹⁴ This indicates that the junctions are approximately optimally damped with McCumber parameters $\beta_c \leq 1$ and $\beta_c \approx 2$ for wafers I and II, respectively.

An SFQ static divider is a useful diagnostic tool for junction properties because it can directly measure the maximum operating frequency (f_{\max}) for a digital circuit. Numerous experiments with static dividers fabricated in Nb/AIO_x/Nb processes^{5,12} show that f_{\max} scales as $\sqrt{J_c}$, at optimum damping of $\beta_c = 1$, as follows:

$$f_{\max} = k \frac{V_c}{\Phi_0} = k \frac{1}{\sqrt{2\pi\Phi_0}} \sqrt{\frac{J_c}{C_f}}, \quad (1)$$

where C_f is the specific capacitance of the junction and $k \approx 0.82$ is an empirical constant. This universal trend is relatively insensitive to the actual value of the damping, although it has not been extensively studied with barrier materials different from AIO_x.

The static divider consists of a voltage-controlled oscillator (VCO), Josephson transmission lines (JTL) interconnecting twelve stages of SFQ toggle flip-flops (TFF), and an output amplifier. The VCO converts a dc input into a SFQ pulse train. The TFF acts as a logical divide-by-two, alternately sending pulses to two output ports. A daisy chain of twelve TFF's divides the VCO frequency by 2^{12} . The divider chain and the VCO are biased independently. An additional independent bias is used for a six-stage JTL buffer in order to

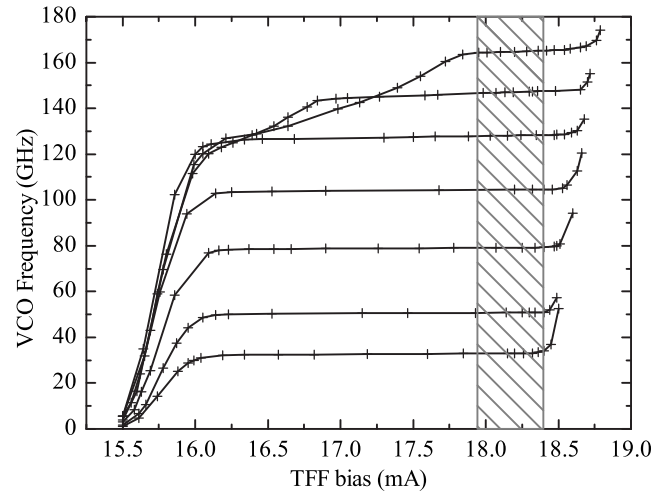


FIG. 2. Measurement of static divider for wafer I. VCO frequency is inferred by multiplying the output frequency by 2^{12} . The circuit shows operating margins up to 165 GHz.

reduce loading effects between the TFF and the VCO. Two additional JTL stages are used between each TFF stage. The last stage is connected to a two-junction comparator that converts the state of the TFF into a voltage, in a manner similar to the SFQ/dc converter described in Ref. 15.

The chip was mounted in a 20 GHz, 24 pad chip holder and cooled to 4.2 K. All lines to the circuit are dc except the output, which is used to apply current and to read voltage through a bias-T at the top of the probe. Results are shown in Fig. 2, in which each set of connected points corresponds to the output frequency of the divider as a function of TFF bias with a fixed operating point of the VCO. The horizontal region of each curve indicates proper digital operation of the divider chain. The observed output frequency is referred back to the VCO pulse train by multiplying by 2^{12} . For fixed TFF bias, the divider chain showed operating margins at all frequencies up to 165 GHz (hashed region in Fig. 2).

The results for these wafers are slightly below the frequency trend determined by Eq. (1) for AIO_x junctions, which indicates a higher C_f for the given J_c . Specifically, the 165 GHz speed of 5.5 kA/cm² NbSi devices compares to the 200 GHz speed for 4.5 kA/cm² AIO_x devices. Assuming that NbSi junctions follow the trend of Eq. (1), C_f must be 100 fF/ μm^2 , compared to 59 fF/ μm^2 for the oxide barrier.¹³ In the future it is important to test NbSi junctions with different J_c s to determine their actual speed performance. Since different compositions and barrier thicknesses can produce similar J_c s, it is possible that the speed scales differently. In addition, a more straightforward test would be to compare externally shunted NbSi junctions with externally shunted AIO_x junctions, in which case C_f should be similar.

Separately, a 16-bit SFQ counter-flow shift register was tested. The design, with 4 junctions per stage (similar to Ref. 16) used parameters identical to a previously tested¹⁷ version of the circuit based on AIO_x junctions. By omitting the external junction shunts, which are unnecessary for these NbSi junctions, the unit-cell area was halved.

Two circuits from each wafer were measured. At the optimum designed bias current of 8.2 mA all circuits showed correct operation with the same experimental bias current margins of about $\pm 30\%$. The measured margins agree with simulated results and are larger than the best reported mar-

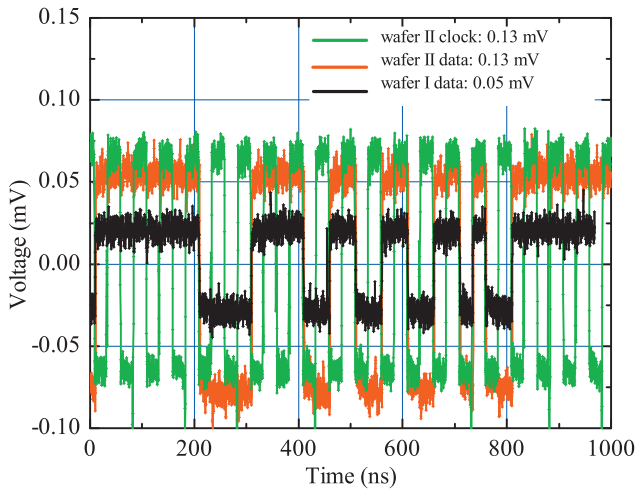


FIG. 3. (Color) Correct output waveforms for the 16 bit shift register for an arbitrary data pattern at 40 Mb/s. The output voltage is 0.05 mV for wafer I and 0.13 mV for wafer II.

gins of $\pm 23\%$ for similar devices based on AlO_x -barrier junctions.¹⁷ The broader operating margins can be attributed to smaller spread in the NbSi junction properties.

The circuit was designed as a low-speed test with standard SFQ/dc converters. The experimentally measured waveforms shown in Fig. 3 were generated by shift register circuits from the two wafers and demonstrate the correct circuit operation. The measured output voltages of 0.05 and 0.13 mV correspond to the dc voltages on single junctions at biases near $1.5I_c$, which agrees with the designed bias and expected output voltage. Output voltages were sufficient for testing the shift registers up to 500 MHz and 1 GHz clock frequency for wafers I and II, respectively.

For $C_f = 100 \text{ fF}/\mu\text{m}^2$, which was estimated using the maximum static divider frequency, and with effective V_c s of 0.37 and 0.67 mV measured from SFQ/dc converters, the effective damping can be estimated to be $\beta_c \approx 0.8$ and $\beta_c \approx 2.6$, which agrees with damping parameters estimated from the I - V curves of single junctions.

The design with self-shunted junctions uses half the area and gives better junction resistance uniformity than externally shunted junctions based on AlO_x barriers. This could be a very important advantage in complex circuits with more

than 10^4 junctions, especially if the improvement persists to higher-speed devices.

This work presents high-yield digital circuits fabricated with intrinsically self-shunted Nb/Nb_xSi_{1-x}/Nb Josephson junctions. The results suggest that NbSi-barrier junctions may be a useful and important junction technology for high-speed digital circuits.

The authors acknowledge useful conversations with H. Rogalla and J. Niemeyer, and the valuable help of G. L. Kerber at JPL. This work was supported in part by the Defense Microelectronics Activity under Contract No. H94003-04-D-0004-0091. U.S. government work, not subjected to U.S. copyright.

¹Superconducting Technology Assessment report (NSA, 2005) online at www.nitrd.gov/PUBS/nsa/sta.pdf.

²M. Gurvitch, M. A. Washington, and H. A. Huggins, *Appl. Phys. Lett.* **42**, 472 (1983).

³R. Pöpel, J. Niemeyer, R. Fromknecht, W. Meier, and L. Grimm, *J. Appl. Phys.* **68**, 4294 (1990).

⁴D. Gupta, T. V. Filippov, A. F. Kirichenko, D. E. Kirichenko, I. V. Vernik, A. Sahu, S. Sarwana, P. Shevchenko, A. Talalaevskii, and O. A. Mukhanov, *IEEE Trans. Appl. Supercond.* **17**, 430 (2007).

⁵S. K. Tolpygo, D. Yohannes, R. T. Hunt, J. Vivalda, D. Donnelly, D. Amparo, and A. F. Kirichenko, *IEEE Trans. Appl. Supercond.* **17**, 946 (2007).

⁶A. W. Kleinsasser, R. E. Miller, W. H. Mallison, and G. B. Arnold, *Phys. Rev. Lett.* **72**, 1738 (1994).

⁷M. Khabipov, D. Balashov, F.-I. Buchholz, and J. Niemeyer, *IEEE Trans. Appl. Supercond.* **11**, 1074 (2001).

⁸F. Mueller, R. Behr, T. Weimann, L. Palafox, D. Olaya, P. D. Dresselhaus, and S. P. Benz, *IEEE Trans. Appl. Supercond.* **19**, 981 (2009).

⁹B. Baek, P. D. Dresselhaus, and S. P. Benz, *IEEE Trans. Appl. Supercond.* **16**, 1966 (2006).

¹⁰D. Olaya, P. D. Dresselhaus, and S. P. Benz, *IEICE Trans. Electron.* **E93-C**, 463 (2010).

¹¹P. D. Dresselhaus, S. P. Benz, C. J. Burroughs, N. F. Bergren, and Y. Chong, *IEEE Trans. Appl. Supercond.* **17**, 173 (2007).

¹²G. L. Kerber, L. A. Abelson, K. Edwards, R. Hu, M. W. Johnson, M. L. Leung, and J. Luine, *IEEE Trans. Appl. Supercond.* **13**, 82 (2003).

¹³Hypres Nb Process Design Rules, (30–1000–4500 A/cm²), online at www.hypres.com.

¹⁴K. K. Likharev, *Dynamics of Josephson Junctions and Circuits* (Gordon and Breach Science, New York, 1986).

¹⁵K. K. Likharev and V. K. Semenov, *IEEE Trans. Appl. Supercond.* **1**, 3 (1991), see Fig. 29.

¹⁶O. A. Mukhanov, *IEEE Trans. Appl. Supercond.* **3**, 2578 (1993).

¹⁷H. Engseth, S. Intiso, M. R. Rafique, E. Tolkacheva, and A. Kidiyarova-Shevchenko, *Supercond. Sci. Technol.* **19**, S376 (2006).